Intrazeolite Metal Carbonyl Kinetics: ^{12}CO Substitution in $Mo(^{12}CO)_6$-$Na_{56}Y$ by PMe_3 and ^{13}CO

Geoffrey A. Ozin,*[a] Saim Özkar,[b] Heloise O. Pastore,[a] Anthony J. Poë*[a] and Eduardo J. S. Vichi[c]

[a] *Lash Miller Chemical Laboratories, University of Toronto, 80 St George Street, Toronto, Ontario, Canada M5S 1A1*
[b] *Department of Chemistry, Middle East Technical University, Ankara, Turkey*
[c] *Instituto de Química, Universidade Estadual de Campinas, Campinas, S. P., Brasil*

The first kinetic study is reported for archetypical substitution reactions of PMe_3 and ^{13}CO with the well defined intrazeolite system, $Mo(^{12}CO)_6$-$Na_{56}Y$, for which excellent isosbestic points and first order behaviour are obtained, the activation parameters indicate a highly ordered 'supramolecular' transition state consisting of activated $Mo(^{12}CO)_6$ and PMe_3 or ^{13}CO all anchored to the Na^+ ions in the α-cage of the host lattice.

The anchoring of metal carbonyls and organometallic compounds to the accessible extraframework 'half-naked' cation sites in zeolite hosts is a ubiquitous phenomenon, with important implications in molecule separation, catalysis and materials science.[1] A range of powerful physical methods is now available to provide detailed structure–bonding information on a variety of intrazeolite guests[2] and a unique opportunity exists to probe reactivity patterns of 'supramolecular guest–host assemblies' through quantitative *in situ* kinetic studies of structurally well characterized 'model' intrazeolite systems. Activation parameters for archetypical intrazeolite metal carbonyl and organometallic transformations could be compared with known values for the same reactions in solution, gas and matrix phases. One could then begin to evaluate intracavity and intrachannel anchoring interactions, space filling constraints, and ordering and cooperative effects that endow the 'nanoreaction chambers' of different zeolite hosts with the special character that they so often display when compared to other supports and other phases.

We present here the first quantitative kinetic results on a well defined intrazeolite metal carbonyl system, namely a phosphine-substitution and a ^{13}CO exchange reaction of $n\{Mo(CO)_6\}$-$Na_{56}Y$, the key structural information for which is summarized in Fig. 1. Briefly, ^{23}Na, ^{13}C and ^{31}P MAS NMR,[3] mid IR and far IR spectroscopy,[4] EXAFS structure determinations,[5] adsorption, and elemental analysis[4,5] have shown saturation loading values in $Na_{56}Y$ of $2Mo(CO)_6$ per α-cage and $4PMe_3$ per α-cage, and these correspond to unit cell formulations of $16\{Mo(CO)_6\}$-$Na_{56}Y$ and $32\{PMe_3\}$-$Na_{56}Y$, respectively (Fig. 1*B,C*). Further, the half-saturation loaded $8\{Mo(CO)_6\}$-$Na_{56}Y$ system (Fig. 1*A*) can additionally adsorb up to an average of $2PMe_3$ per α-cage to yield $8\{Mo(CO)_6\},16\{PMe_3\}$-$Na_{56}Y$ (Fig. 1*D*). The four site II

Na^+ ions are tetrahedrally organized in the supercage of $Na_{56}Y^{4-6}$ and can trap a single $Mo(CO)_6$ molecule and two $2PMe_3$ ligands in the arrangement sketched in Fig. 1*D*. The IR spectrum indicates that the $Mo(CO)_6$ is no longer strongly anchored to extraframework Na^+ ions, a situation that is also apparent for $n\{Mo(CO)_6\},m\{^{13}CO\}$-$Na_{56}Y$. Full details of our combined intrazeolite kinetics cell and Fourier transform mid IR detection system will be presented elsewhere.[7] The key results of our first kinetic study in this important new field are reported below.

Hexacarbonylmolybdenum(0) in the 13 Å-diameter supercage void system of dehydrated sodium zeolite Y, $n\{Mo(CO)_6\}$-$Na_{56}Y$ ($n < 8$), undergoes ^{12}CO substitution reactions in the presence of trimethylphosphine in $n\{Mo(CO)_6\},m\{PMe_3\}$-$Na_{56}Y$, or of isotopically labelled carbon monoxide in $n\{Mo(CO)_6\},m\{^{13}CO\}$-$Na_{56}Y$, to afford intrazeolite, *cis*-$\{Mo(^{12}CO)_4(PMe_3)_2\}$-$Na_{56}Y$, and fully labelled $\{Mo(^{13}CO)_6\}$-$Na_{56}Y$, respectively. No reaction intermediates were detected in the PMe_3 system, as suggested by the excellent isosbestic point in Fig. 2. Non-involvement of $Mo(^{12}CO)_5PMe_3$ was confirmed by direct impregnation of $Mo(^{12}CO)_5(PMe_3)$, and the demonstration that this reacts much more slowly than $Mo(CO)_6$.

These reactions proceed by very well behaved first order processes (Fig. 3*a*) that involve what we believe to be a supramolecular assembly of $Mo(^{12}CO)_6$, PMe_3 or ^{13}CO ligands, and extraframework Na^+ ions, all housed together in the supercage of $Na_{56}Y$ as illustrated for $8\{Mo(^{12}CO)_6\},16\{PMe_3\}$-$Na_{56}Y$ in Fig. 1*D*. The observed rate constants $k_{obs}(PMe_3)$ and $k_{obs}(^{13}CO)$ lie between 8.31×10^{-5} and 1.19×10^{-3} s^{-1}, and 9.10×10^{-5} and 1.11×10^{-3} s^{-1}, respectively, in the temperature range 45–95 °C. Excellent Eyring plots (Fig. 3*b*) yield activation parameters shown in Table 1. The values of $\Delta H^{\ddagger}$ are between 60 and 90 kJ mol^{-1} smaller than those found for similar types of reactions in the solution and gas phase,[8] respectively (Table 1). This dramatic decrease, for what we describe as 'intracage' first-order dissociative ^{12}CO substitution reactions, is believed to originate in much stronger cation anchoring of the $\{Mo(^{12}CO)_5\cdots(^{12}CO)\}^{\ddagger}$ transition state compared with that of the ground state $Mo(^{12}CO)_6$. This also could account for the large negative values for $\Delta S^{\ddagger}$ since the much more weakly anchored $Mo(^{12}CO)_6$ in the ground state is transformed by CO dissociation into the tightly anchored† $Mo(^{12}CO)_5$ intermediate, this transformation being associated with increased back-bonding in the less highly coordinated intermediate, and the consequently greater negative charge on the oxygen atoms of the carbonyl ligands. The 'kinetic signature' provided by this study complements, supports and amplifies the 'spectroscopic–structure–bonding' picture for $n\{Mo(^{12}CO)_6\}$-$Na_{56}Y$ derived from earlier studies.[3–5]

The closeness of the $\Delta H^{\ddagger}$ and $\Delta S^{\ddagger}$ values for the intrazeolite PMe_3 and ^{13}CO reactions demonstrates the mechanistic similarities of the two processes. The observed rates are controlled by the dissociative loss of the first ^{12}CO from

Table 1 Activation parameters for dissociative reactions of $Mo(CO)_6$

Entering Ligand	Medium	$\Delta H^{\ddagger}$/ kJ mol^{-1}	$\Delta S^{\ddagger}$/ J K^{-1} mol^{-1}
None[a]	Gas phase	157	38
^{14}CO[b]	Gas phase	126.4	−1.7
$PBu^n{}_3$[b]	Decalin	132.5	28
PMe_3	$Na_{56}Y$	69.5	−106.8
^{13}CO[c]	$Na_{56}Y$	65.3	−126.8

[a] Irreversible CO loss induced by pulsed laser pyrolysis technique at 670–760 K; ref. 8(*c*). [b] Ref. 8(*b*). [c] $P(^{13}CO)$ = 100 Torr.

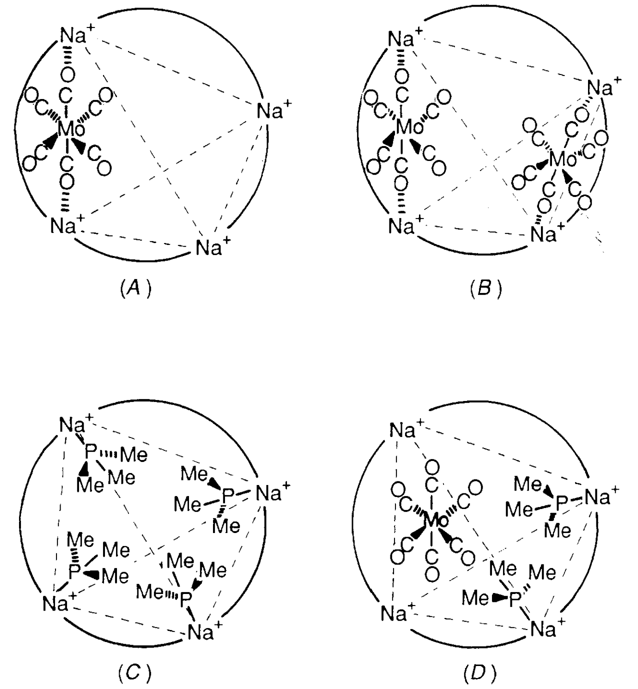

Fig. 1 Summary of structural data for (*A*) $8\{Mo(CO)_6\}$-$Na_{56}Y$, (*B*) $16\{Mo(CO)_6\}$-$Na_{56}Y$, (*C*) $32\{PMe_3\}$-$Na_{56}Y$ and (*D*) $8\{Mo(CO)_6\},16\{PMe_3\}$-$Na_{56}Y$

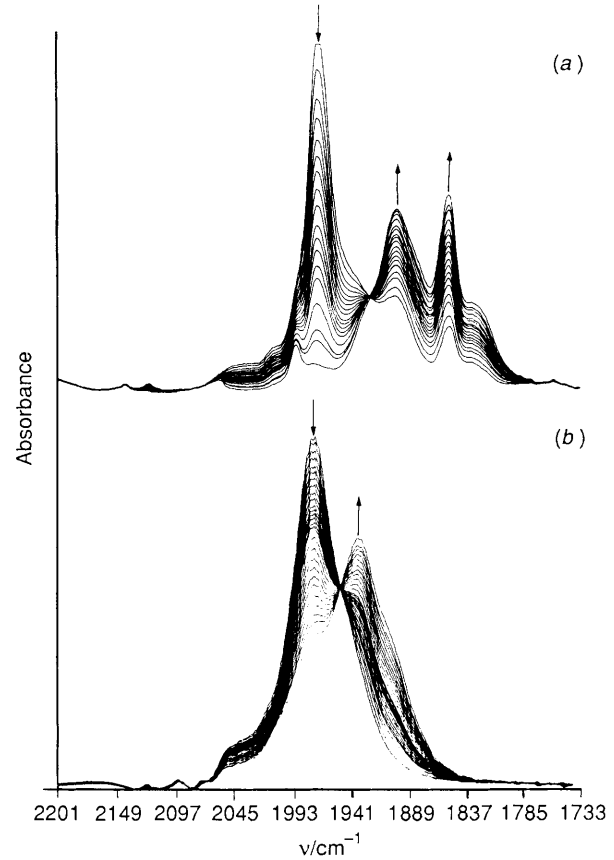

Fig. 2 Typical mid IR spectral changes observed for (*a*) $n\{Mo(^{12}CO)_6\},m\{PMe_3\}$-$Na_{56}Y$ and (*b*) $n\{Mo(^{12}CO)_6\},m\{^{13}CO\}$-$Na_{56}Y$ [$P(^{13}CO)$ = 100 Torr), T = 65.8 °C]

---

† A similar explanation involving a tightening up of the transition state has been offered for a negative (−89 J K^{-1} mol^{-1}) value of $\Delta S^{\ddagger}$ observed for a CO dissociative reaction of $Ru_3(CO)_9(PBu^n{}_3)_3$ in decalin (S. K. Malik and A. J. Poë, *Inorg. Chem.*, 1979, **18**, 1241).

$$\{Mo(CO)_6\}\text{-}NaOZ \underset{k_{-1}}{\overset{k_1}{\rightleftarrows}} ZONa\cdots(OC)Mo(CO)_3(CO)\cdots NaOZ + CO \tag{1}$$

$$ZONa\cdots(OC)Mo(CO)_3(CO)\cdots NaOZ \overset{k_2}{\rightleftarrows} ZONa\cdots(OC)Mo(CO)_2(CO)\cdots NaOZ + CO \tag{2}$$

$$ZONa\cdots(OC)Mo(CO)_2(CO)\cdots NaOZ + ZONa\cdots PMe_3 \rightarrow ZONa\cdots(OC)Mo(CO)_2(PMe_3)(CO)\cdots NaOZ \tag{3}$$

$$ZONa\cdots(OC)Mo(CO)_2(PMe_3)(CO)\cdots NaOZ + ZONa\cdots PMe_3 \rightarrow ZONa\cdots(OC)Mo(CO)_2(PMe_3)_2(CO)\cdots NaOZ \tag{4}$$

$$ZONa\cdots(OC)Mo(CO)_2(CO)\cdots NaOZ + 4\,{}^{13}CO \rightleftarrows\rightleftarrows\rightleftarrows\rightleftarrows ZONa\cdots(O^{13}C)Mo({}^{13}CO)_2({}^{13}CO)\cdots NaOZ + 4\,{}^{12}CO \tag{5}$$

$$ZONa\cdots(O^{13}C)Mo({}^{13}CO)_2({}^{13}CO)\cdots NaOZ + {}^{13}CO \rightarrow NaOZ\cdots(O^{13}C)Mo({}^{13}CO)_3({}^{13}CO)\cdots NaOZ \tag{6}$$

$$ZONa\cdots(O^{13}C)Mo({}^{13}CO)_3({}^{13}CO)\cdots NaOZ + {}^{13}CO \rightarrow NaOZ\cdots(O^{13}C)Mo({}^{13}CO)_4({}^{13}CO)\cdots NaOZ \tag{7}$$

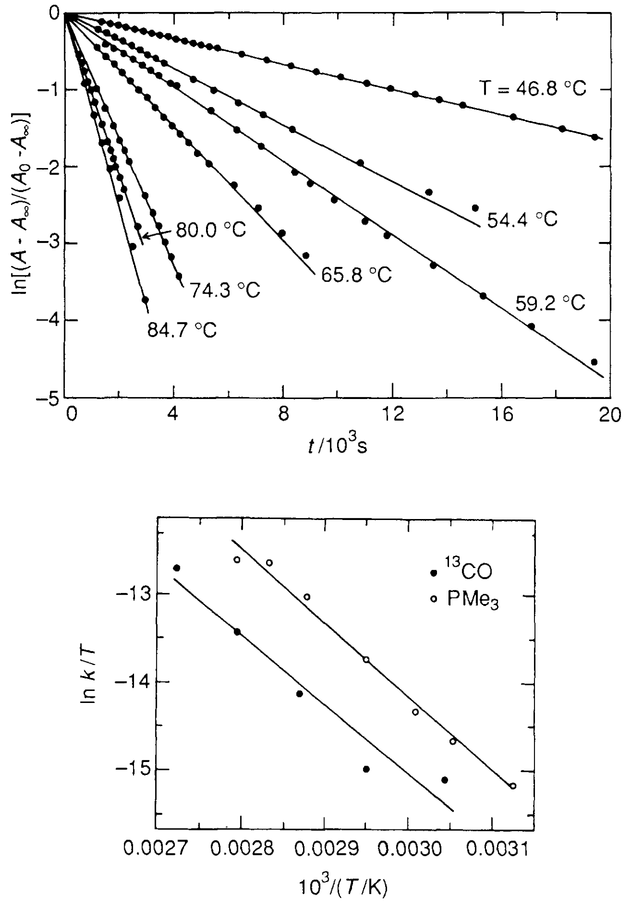

Fig. 3 (*a*) First order plots for reactions with PMe_3, and (*b*) Eyring plots for reactions with PMe_3 and ^{13}CO [$P(^{13}CO)$ = 100 Torr]

$Mo(^{12}CO)_6$ although the energetics of this step can probably be modified by effects transmitted through the zeolite from the entering groups that are initially anchored to the accessible extraframework Na^+ ions. In the case of PMe_3, the kinetic data are consistent with the sequence of reactions (1)–(4). In the absence of added CO, $k_2 >> k_{-1}[CO]$ or k_1 and the rate determining step is simply the forward reaction in eqn. (1).

When the entering ligand is ^{13}CO, the kinetic data are consistent with a similar reaction sequence except that a series of rapid $^{12}CO/^{13}CO$ exchange reactions precede steps analogous to (3) and (4) according to the reactions shown in eqn. (5)–(7) to yield the major product $\{Mo(^{13}CO)_6\}\text{-}Na_{56}Y$.

Extensive studies involving variation in $Mo(^{12}CO)_6$ and PMe_3 loading, ^{12}CO and ^{13}CO pressure, the nature of mono- and bi-dentate phosphine reactants, extraframework cations, Si/Al ratio, zeolite structure type, and temperature are under way.[7] These results will allow us to assemble a comprehensive and quantitative mechanistic picture for these important archetypical intrazeolite metal carbonyl reactions.

The financial assistance of the Natural Sciences and Engineering Research Council of Canada (G. A. O., A. J. P.) is appreciated. S.O. is indebted to the Middle East Technical University, Ankara, for leave of absence and H. O. P. and E. J. S. V. acknowledge CNPq (Brasil) and FAPESP (Sao Paulo) for a graduate scholarship (H. O. P.) and financial support (E. J. S. V.).

Received, 28th August 1990; Com. 0/03886E

References

1 G. A. Ozin and C. Gil, *Chem. Rev.*, 1989, **89**, 1749; G. A. Ozin and S. Özkar, *Acc. Chem. Res.*, submitted for publication; G. A. Ozin, A. Stein and A. Kuperman, *Angew. Chem., Int. Ed. Engl.* (*Adv. Mat.*), 1989, **101**, 373; G. D. Stucky and J. MacDougall, *Science*, 1990, **247**, 669, and references cited therein.
2 J. M. Thomas and D. E. W. Vaughan, *J. Phys. Chem. Solids*, 1989, **50**, 449; J. M. Thomas, in *Zeolites: Facts, Figures, Future*, eds. P. A. Jacobs and R. A. van Santem, Elsevier, Amsterdam, 1989.
3 G. A. Ozin, S. Özkar and P. M. Macdonald, *J. Phys. Chem.*, 1990, **94**, 6939; G. A. Ozin and S. Özkar, *J. Phys. Chem.*, 1990, **94**, 7556.
4 G. A. Ozin, S. Özkar, T. Bein and K. Moller, *J. Am. Chem. Soc.*, in the press.
5 S. Özkar, G. A. Ozin, T. Bein and K. Moller, *J. Phys. Chem.*, submitted for publication; J. M. Coddington, R. F. Howe, Y. S. Yong, K. Asakura and Y. Iwasawa, *J. Chem. Soc., Faraday Trans.*, 1990, **86**, 1015, and references cited therein.
6 A. N. Fitch, H. Jobic and A. Renouprez, *J. Phys. Chem.*, 1986, **90**, 1311.
7 G. A. Ozin, S. Özkar, H. O. Pastore, A. J. Poë and E. J. S. Vichi, to be published.
8 (*a*) J. M. Morse, H. P. Gregory and T. J. Burkey, *Organometallics*, 1989, **8**, 2471; (*b*) J. A. S. Howell and P. M. Burkinshaw, *Chem. Rev.*, 1983, **83**, 557; (*c*) K. E. Lewis, D. M. Golden and G. P. Smith, *J. Am. Chem. Soc.*, 1984, **106**, 3905, and references cited therein.